Soft Scattering Re-Visited

Uri MAOR

Tel-Aviv University

EDS'09, CERN Genève

Soft Scattering Re-Visited

Uri MAOR
Tel-Aviv University

EDS'09, CERN Geneve

1. Introduction

The renewed interest in soft scattring and Pomeron physics, which was dormant for many years, is correlated to the market demand for reliable estimates of hard diffraction gap survival probabilities, notably diffractive Higgs production at the LHC.

It is interesting to note that the present rigorous study of this subject is mostly based on sophisticated utilizations of relatively old theoretical ideas and models, notably Gribov's Reggeon field theory and eikonal models which enable us to secure that a Regge type parameterization with $\alpha_{I\!P}(0) = 1+\Delta_{I\!P} > 1$ is compatible with **s and t channel unitarity**. Specifically, a given Pomeron trajectory with $\alpha_{I\!P}(t) = 1+\Delta_{I\!P}+\alpha'_{I\!P}t$ implies a violation of s-channel unitarity at high enough energies. The implementation of s-channel unitarity constraints is **model dependent**. In this talk I shall confine myself to the analysis of eikonal models since they have the virtue of simplicity.

t-channel unitarity is intimately connected with the introduction of multi Pomeron interactions ($I\!P$ enhancement). This is a consequence of Mueller's triple Pomeron mechanism coupled to the ISR/CDF analysis implying that $G_{3I\!P}$ is relatively large.

Recall that in the ISR-Tevatron energy range σ_{tot} and σ_{el} are well reproduced with Donnachie-Landshoff $\Delta \simeq 0.08$ and $\alpha'_{I\!P} \simeq 0.25\ GeV^{-2}$. The energy dependence of the soft diffractive channels is much milder. Notably, the energy dependence of σ_{sd} is very mild implying that strong screening initiated by s-unitarity must be taken into account.

This observation is accompanied by the dynamical need to differentiate between low mass diffraction associated with the Good-Walker mechanism and high mass diffraction initiated by Pomeron enhancement.

I shall discuss the modelling of the above dynamical observations with special emphesis on:

- The implications of s-channel screening and Pomeron enhancement on soft scattering and its implied gap survival probabilities.
- The approach of the elastic amplitude, at small impact parameter b, toward the black disc bound.
- How much diffraction (soft and hard) do we expect at exceedingly high energies.
- The interplay between theory and data analysis in soft scattering modellings.
- The identification of experimental signatures implied by the above.
- The nature of the Pomeron and its QCD foundations. What is the relation between soft and hard Pomerons?

2. The Good-Walker Eikonal Models

Updated eikonal models are multichannel, taking into account both elastic and diffractive re-scatterings. This is a consequence of the Good-Walker mechanism.

Consider a system with 2 states: a hadron $|h\rangle$ and a diffractive system $|D\rangle$. The GW mechanism stems from the observation that these states do not diagonalize the 2×2 scattering matrix $\mathbf{T}$. Define the eigen states of $\mathbf{T}$ by $|\psi_1\rangle$ and $|\psi_2\rangle$. We obtain

$$\psi_h = \alpha\psi_1 + \beta\psi_2 \qquad \alpha^2+\beta^2=1$$
$$\psi_D = -\beta\psi_1 + \alpha\psi_2$$

In this representation we consider 4 elastic scatterings of ψ_i and ψ_k $(i,k=1,2)$: $A_{i,k} = \langle\psi_i\psi_k|\mathbf{T}|\psi_i\psi_k\rangle$.

In pp and $\bar{p}p$ scattering $A_{1,2} = A_{2,1}$ and we have 3 independent amplitudes which are the building blocks of:

$A_{i,k} = A_{i,k}(s,b)$

$$a_{el}(s,b) = i\{\alpha^4 A_{1,1} + 2\alpha^2\beta^2 A_{1,2} + \beta^4 A_{2,2}\}$$
$$a_{sd}(s,b) = i\alpha\beta\{-\alpha^2 A_{1,1} + (\alpha^2-\beta^2)A_{1,2} + \beta^2 A_{2,2}\}$$
$$a_{dd}(s,b) = i\alpha^2\beta^2\{A_{1,1} - 2A_{1,2} + A_{2,2}\}$$

Specification of a_{el}, a_{SD} and a_{DD} enables us to calculate through a b integration the total cross section and the differential and integrated elastic, SD and DD cross sections.

For each of the $A_{i,\lambda}$ amplitudes we write its unitarity equation $2\,\mathrm{Im}\,A_{i,\lambda}(s,b) = |A_{i,\lambda}(s,b)|^2 + G^{in}_{i,\lambda}(s,b)$. i.e. for each i,λ

$$\sigma_{tot}^{i,\lambda}(s,b) = \sigma_{el}^{i,\lambda}(s,b) + \sigma_{in}^{i,\lambda}(s,b)$$

A general solution can be written as $A_{i,\lambda} = i\left(1 - e^{-\frac{1}{2}\Omega_{i,\lambda}}\right)$

$G^{in}_{i,\lambda} = 1 - e^{-\Omega(s,b)}$. In the eikonal approximation we assume that $A_{i,\lambda}(s,b)$ is imaginary (i.e. $\Omega_{i,\lambda}$ is real). $\Omega_{i,\lambda}(s,b)$ is determined by the input model.

$\Rightarrow P_{i,\lambda}(s,b) = e^{-\Omega(s,b)}$ is the probability that the GW (i,λ) projectiles will reach the final non GW interaction in their initial state, regardless of their prior re-scattering.

Eikonal models based on the GW mechanism use a Regge like formalism in which the soft Pomeron trajectory is $\alpha_{I\!P}(t) = 1 + \Delta_{I\!P} + \alpha'_{I\!P} t$. The corresponding opacity is $\Omega_{ij,k\ell}(s,b) = \nu_{ij,k\ell}(s)\, \Gamma_{ij,k\ell}(s,b;\alpha'_{I\!P})$ where $\nu_{ij,k\ell} = g_i g_\ell \left(\frac{s}{s_0}\right)^{\Delta_{I\!P}}$.
$\Gamma_{ij,k\ell}$ are the b-profiles of the $(ij,k\ell)$ elastic scatterings.
Recall that $1-e^{-x} = x - \frac{x^2}{2!} + \frac{x^3}{3!} - \ldots$ $(ij,k\ell = pp)$. Consequently

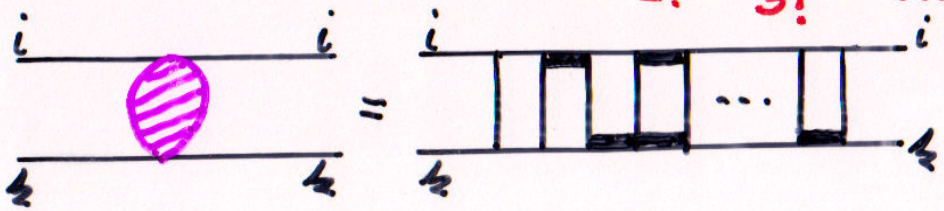

. $\Gamma_{ij,k\ell}(s,b)$ is external information derived from a fit to the soft scattering data, essentially the differential cross sections.

In GLMM(08) the b-profiles are given by a 2-pole in t-space

$$\Gamma_{ij,k\ell}(t; m_i, m_{k\ell}) = \frac{1}{(1 - t/m_i^2)} \times \frac{1}{(1 - t/m_{k\ell}^2)} \Longrightarrow \Gamma_{ij,k\ell}(b; m_i, m_{k\ell})$$

to which we introduce a mild energy dependence

$$m^2 \Longrightarrow m^2(s) = \frac{m^2}{1 + \frac{m^2}{4}\alpha'_{I\!P} \ln\frac{s}{s_0}}$$. This parametrization is compatible with the requirements of analiticity/crossing at large b, pQCD at large t, Regge at small t.

KMR b-profiles are formulated some what differently than ours, but numerically they are similar.

Consider a model in which diffraction is exclusively GW. This was recently considered by GLM(08), GLMM(09) and LKMR(08). All these GW models fit their (different!) elastic sectors of their data bases with $\frac{\chi^2}{d.o.f} < 1.0$ with fitted $\Delta_{I\!P} = 0.10 - 0.12$ and $\alpha'_{I\!P} = 0.012 - 0.066$.

The above GW models fail to reproduce the diffractive sectors of their data base. This deficiency is traced to high mass diffraction which is mostly non GW.

3. Multi Pomeron Interactions

- Mueller (1969) triple Pomeron diagram (derived from 3 body unitarity)

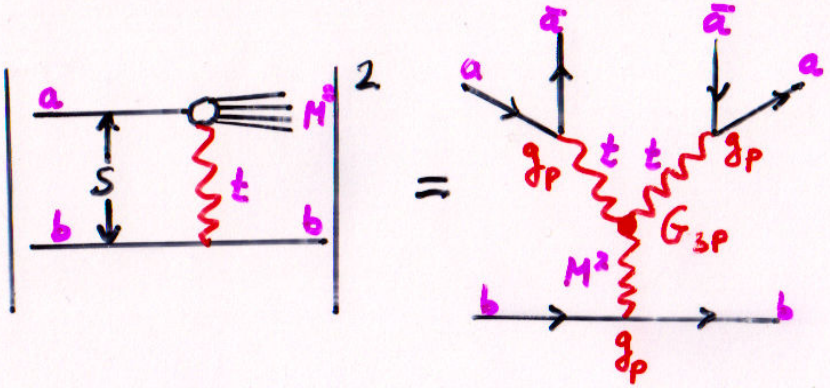

leads to high mass diffraction which is non GW. Recall that

$\frac{M^2}{s} \leq 0.05$ (commonly used but arbitrary)

The approximation requires that $M^2 \gg m_p^2$.

$$M^2 \frac{d\sigma^{3P}}{dt\,dM^2} = \frac{1}{16\pi^2} g_p^2(t)\, g_p(0)\, G_{3P}(t) \left(\frac{s}{M^2}\right)^{2\Delta_p + 2\alpha_p' t} \left(\frac{M^2}{s_0}\right)^{\Delta_p} + \text{secondary terms}$$

- CDF analysis suggests a relatively high value of G_{3P}.
- Assume G_{3P} is not too small $\Rightarrow$ we need to consider a very large family of multi Pomeron interactions (IP enhancement) which are not included in the GW mechanism.
- As we shall see, this "new" dynamical mechanism initiates profound differences in the calculated values of soft diffractive cross sections and survival probabilities of non GW diffractive channels (soft and hard). These differences are significant at high energies above the Tevatron !!!

	$\Delta_{I\!P}$	β	$\alpha'_{I\!P}$	g_1	g_2	m_2	m_1	χ^2/d.o.f.
GW	0.120	0.46	0.012 GeV^{-2}	1.27 GeV^{-1}	3.33 GeV^{-1}	0.913 GeV	0.98 GeV	0.87
GW+$I\!P$-enhanced	0.335	0.34	0.010 GeV^{-2}	5.82 GeV^{-1}	239.6 GeV^{-1}	1.54 GeV	3.06 GeV	1.00

TABLE I: Fitted parameters for GLMM(08) GW and GW+$I\!P$-enhanced models.

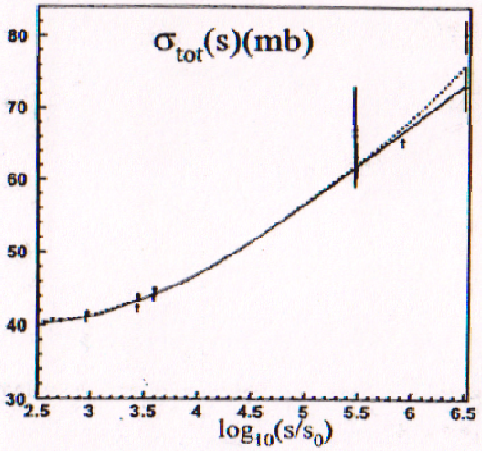

Figure 1: Energy dependence of σ_{tot}. The solid line shows the fit with taking into account all Pomeron interactions while the dashed line corresponds to two channel (eikonal) model.

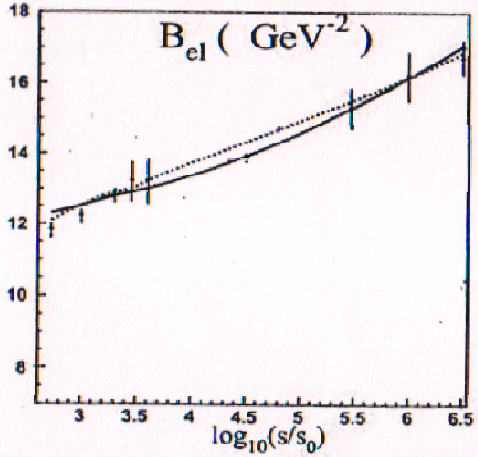

Figure 2: Energy dependence of the slope for the differential elastic cross section. All notation are the same as in Fig. 1

$p\bar{p}$

As noted, the Tel-Aviv and Durham models are conceptually similar. Both utilize multi channel eikonal models so as to be compatible with s-channel unitarity and multi Pomeron interactions so as to be compatible with t- channel unitarity. Their output, though, is significantly different reflecting both different modellings and data analysis.

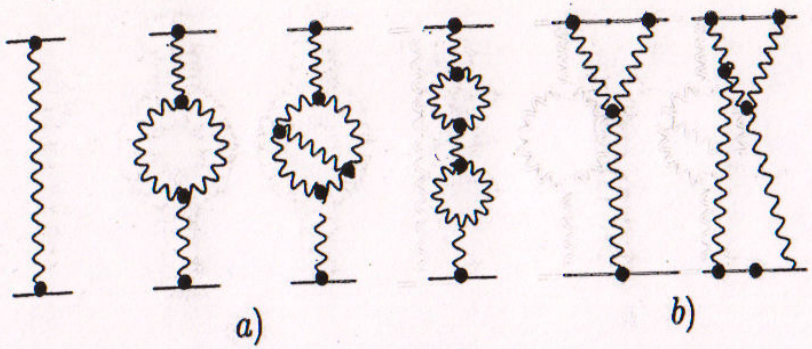

FIG. 1: Typical low order terms of the Pomeron Green's function. Enhanced Pomeron diagrams are shown in Fig. 1a, whereas Fig. 1b shows semi-enhanced diagrams which are not included in our calculations as yet.

Pomeron enhancement initiates changes in the calculated cross sections and gap survival probabilities. We distinguish between enhanced and semi-enhanced diagrams.

- On the one hand, this dynamics adds an additional integration over the rapidity of the 3P vertex. This integration enhances the 3P contribution logarithmically. Hence, an increase of the diffractive high mass cross sections.
- On the other hand, this dynamics initiates both vertex and propagator renormalizations which reduce the effective value of Δ_P. This effect is reasonably small in the ISR - Tevatron range, but it becomes significant in LHC and above.

	Δ_P^{input}	Δ_P^{SSS} 1.8 - 14	Δ_P^{SSS} 14 - 100	σ_{tot} LHC	σ_{el} LHC	σ_{sd} LHC
GLMM(08)	0.335	0.056	0.041	92.1	20.9	11.8
KMR(07)	0.55	0.042	0.027	88.0	20.1	13.3
KMR(08)	0.30	0.053	0.042	91.7	20.9	19.0
LKMR(09)	0.121	0.064		95.0		
GLM(07)	0.15	0.085	0.079	110.5	25.3	11.6

- In general, the output dependence of σ_{tot}, σ_{ee}, σ_{sd}, σ_{dd}, B_{ee} on energy are obtained through a balanced act between Δ_{IP} and α'_{IP} inputs. The smaller α'_{IP} gets, a larger Δ_P is needed to reproduce the experimentally observed shrinkage of $\frac{d\sigma_{ee}}{dt}$ in the forward cone. A signature of the models just compared is that the rate at which B_{ee} is increased with energy is getting slower than predicted by a bare Regge formalism such as DL.
- In addition to the cross section reduction resulting from the renormalization of the Pomeron contribution, the Pomeron enhanced dynamics further reduces the gap survival probabilities initiated by the rescatterings of the incoming projectiles. Recall that gap survival probabilities apply to all non GW diffractive channels (soft and hard) including high mass diffraction. (Details in Gotsman's talk).

4. Same Concept - Different Models

GLMM(08) and KMR(07) treatment of multi-Pomeron interactions (Pomeron enhanced) stems from a few classical papers on this subject notably Kaidalov, Ponomarev, Ter-Martirosyan (1986). At the core of these papers is Gribov's Reggeon Calculus and its partonic interpretation. Recall that in our context the soft Pomeron is a simple pole in the J-plane, while the hard (BFKL?) Pomeron is a branch cut.

- KMR(07) derives directly from these foundations. At the foundation of the KMR(07) model are 2 ad hoc assumptions.

1) The coupling of a multi Pomeron point vertex $n\mathbb{P} \to m\mathbb{P}$ $(n+m \geq 3)$ is $g_m^n = \frac{1}{2} g_N\, nm\, \lambda^{n+m-2}$ $(n+m \geq 3)$. In this notation $G_{3P} = \lambda g_N$.
This assumption is not supported by either decisive data or a theoretical proof and it is justified by claiming it is "reasonable". Note that in Kaidalov et.al. $g_m^n = \frac{1}{2} g_N \lambda^{n+m-2}$, i.e. it is considerably smaller. High order g_m^n couplings are needed to avoid pathological reduction of Δ_P below 1. I shall discuss it in conjunction to the GLMM model.

2) Most of LHC non GW diffractive reaction of interest are hard. Given a triple $I\!P$ bare coupling  we recall that $G_{3I\!P}$ was originally defined for 3 soft $I\!P$. KMR assume that $G_{3I\!P}$ does not change by the interchange of **soft → hard**. This is not self evident.

- The key observation of GLMM(08) is that the exceedingly small fitted $\alpha'_{I\!P} = 0.01\ \text{GeV}^{-2}$ implies that the "soft Pomeron" is hard enough to be treated perturbatively. Following Gribov we identify a correlation between $\alpha'_{I\!P}$ and $\langle p_t \rangle$, the mean **transverse momentum of the partons (actually colour dipoles) associated with the $I\!P$.** Recall that the smallness of $\alpha'_{I\!P}$ is a general feature of GLMM and KMR models.

	GLMM(08)	KMR(07)	KMR(08)
$\Delta_{I\!P}$	0.335	0.55	0.30
$\alpha'_{I\!P}$	0.010	0	0.05

GLMM(08): $\langle p_t \rangle = 1/\sqrt{\alpha'_{I\!P}} \simeq 10\ \text{GeV}$

$\Rightarrow$ QCD running coupling constant is small enough to enable a pQCD calculation. $\alpha_s \propto \ln\left(\langle p_t^2 \rangle / \Lambda^2_{QCD}\right) \ll 1$.

Technically, we have adopted the pQCD MPSI procedure. In this summation g_m^n is reduced to a sequence of triple $I\!P$ vertexes (Fan diagrams). For this calculation we need to calculate the probabilities for $I\!P \to 2I\!P$ (pair production) and $2I\!P \to I\!P$ (annihilation).

Alan Martin has been very critical of the GLMM model presenting his opinion in several meetings over the last 2 years. According to him the lack of explicit b-dependence in MPSI approximation and the lack of direct point like multi Pomeron couplings in which $n+m>3$, contradict the asymptotic dependence of σ_{tot} in the $s\to\infty$ limit obtained from general principles. Specifically, $\Delta_{I\!P}^{eff}$ becomes negative at high enough energies. Regardless of the technical details, Alan's claim is conseptually non relevant! We have no tools to predict the functional transition from pre asymptotic to asymptotic energies. Both the GLMM and KMR have a bound of validity at $W=100\,TeV$. This bound is a consequence of both groups executing their calculations with $\alpha'_{I\!P}=0$ (which is a more severe crime than what we are accused of). As it stands, $\Delta_{I\!P}^{eff}(GLMM(08)) > \Delta_{I\!P}^{eff}(KMR(07))$ and $\Delta_{I\!P}^{eff}(GLMM(08)) \geq \Delta_{I\!P}^{eff}(KMR(08))$. The above holds up to $W=100\,TeV$.

Following is a comparison of the output of Tel-Aviv and Durham.

KMR (00) GW

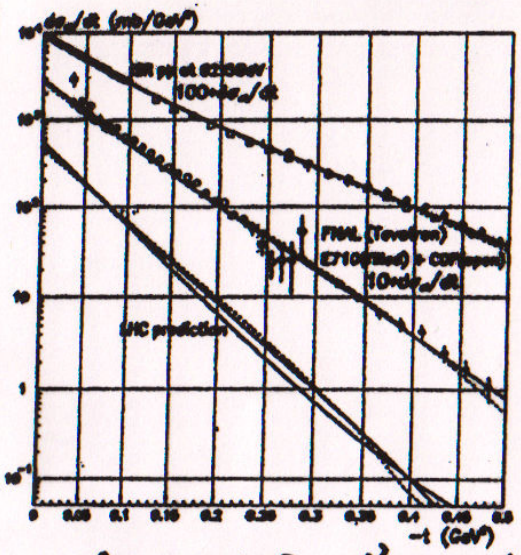

$\Delta_{I\!P} = 0.102 \quad \alpha'_{I\!P} = 0.066$

RMK (07)

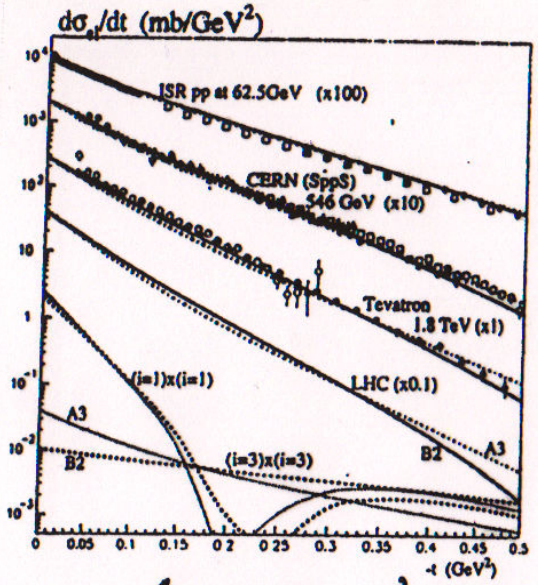

$\Delta_{I\!P} = 0.55 \quad \alpha'_{I\!P} \equiv 0$

RMK (08)

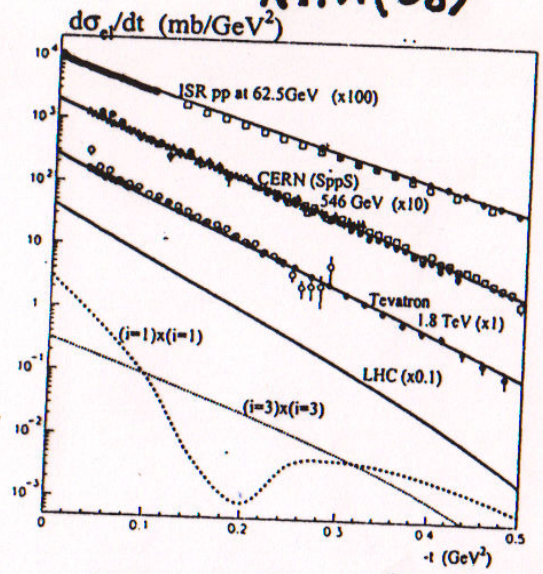

$\Delta_{I\!P} = 0.30 \quad \alpha'_{I\!P} = 0.05$

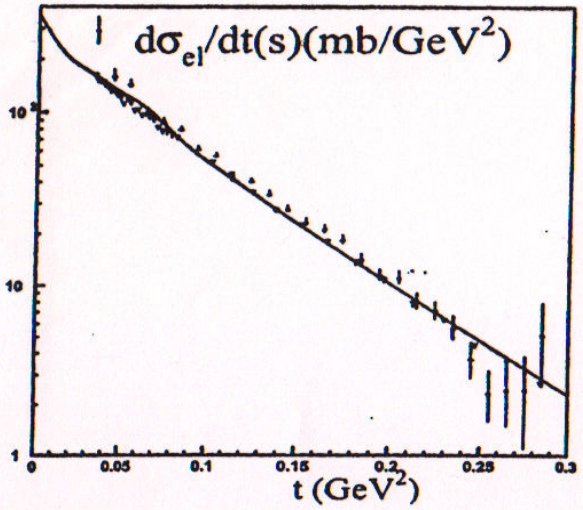

GLMM (08) GW

$\Delta_{I\!P} = 0.12$

$\alpha'_{I\!P} = 0.012$

GLMM (08) GW+$I\!P$enh

$\Delta_{I\!P} = 0.335$

$\alpha'_{I\!P} = 0.010$

LKMR (08)

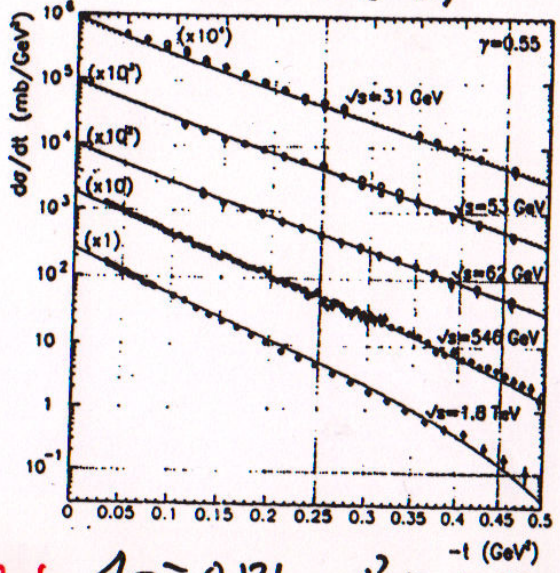

$\Delta_{I\!P} = 0.121 \quad \alpha'_{I\!P} = 0.033$

The 5 models displayed have similar b-profiles!

1) σ_{tot}, σ_{el}, $\frac{d\sigma_{el}}{dt}$ are compatible.

2) KMR estimates of σ_{sd} are larger than GLMM.

3) The incompatability between GLMM and KMR becomes extreme when comparing σ_{dd}.

4) In early publications KMR had $\sigma_{dd} > \sigma_{sd}$. In the latest set of papers the high mass sector of σ_{dd} is omitted!

	Tevatron			LHC			W=10^5 GeV		
	GLMM	KMR(07)	KMR(08)	GLMM	KMR(07)	KMR(08)	GLMM	KMR(07)	KMR(08)
σ_{tot}(mb)	73.3	74.0	73.7	92.1	88.0	91.7	108.0	98.0	108.0
σ_{el}(mb)	16.3	16.3	16.4	20.9	20.1	21.5	24.0	22.9	26.2
σ_{sd}(mb)	9.8	10.9	13.8	11.8	13.3	19.0	14.4	15.7	24.2
$\sigma_{sd}^{\text{low M}}$	8.6	4.4	4.1	10.5	5.1	4.9	12.2	5.7	5.6
$\sigma_{sd}^{\text{high M}}$	1.2	6.5	9.7	1.3	8.2	14.1	2.2	10.0	18.6
σ_{dd}(mb)	5.4	7.2		6.1	13.4	?	6.3	17.3	
$\frac{\sigma_{el}+\sigma_{diff}}{\sigma_{tot}}$	0.43	0.46		0.42	0.53	?	0.41	0.57	

TABLE III: Comparison of GLMM, KMR(07) and KMR(08) outputs.

5) The extensive LKMR(09) analysis of $\frac{d\sigma_{sd}}{dt\, d\frac{M^2}{s}}$ convincingly demonstrates the need to supplement the 3P vertex with secondary Regge contributions such as PPR and RRP. LKMR addresses the Pomeron enhanced contribution only at its lowest order. As such this analysis has very limited relevance in our context.

6) KMR(07) and GLMM(08) calculations of $\frac{d\sigma_{sd}}{dt\, d\frac{M^2}{s}}$ are consistency checks as both models need an arbitrary background term so as to reproduce the CDF data.

7) Note that LKMR(09) were able to fit the data at 540 and 1800 GeV only after a relative normalization rescale of 25%.

$1 - X_L = \frac{M_{sd}^2}{s}$

GLMM (08) $\mathbb{P}$ enhanced + GW

$\Delta_{\mathbb{P}} = 0.335 \quad \alpha'_{\mathbb{P}} = 0.010$

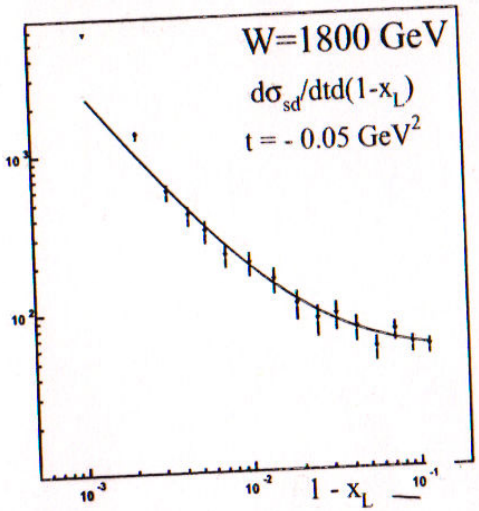

LKMR (08)

GW + Mueller's 3$\mathbb{P}$ SD only

$\Delta_{\mathbb{P}} = 0.121 \quad \alpha'_{\mathbb{P}} = 0.033$

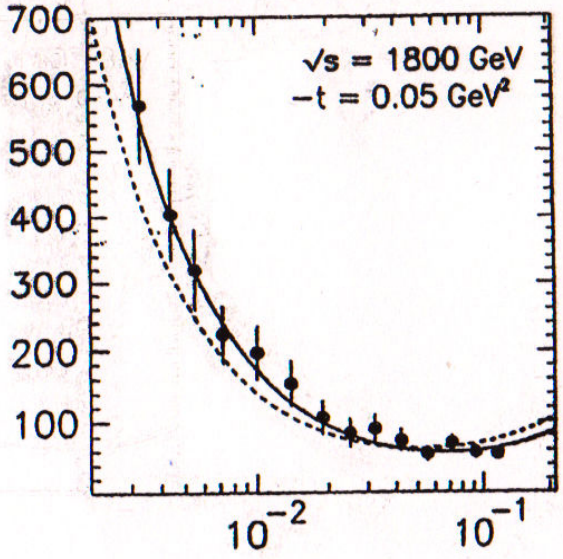

KMR (07)

$\mathbb{P}$ enhanced + GW

$\Delta_{\mathbb{P}} = 0.55 \quad \alpha'_{\mathbb{P}} \equiv 0$

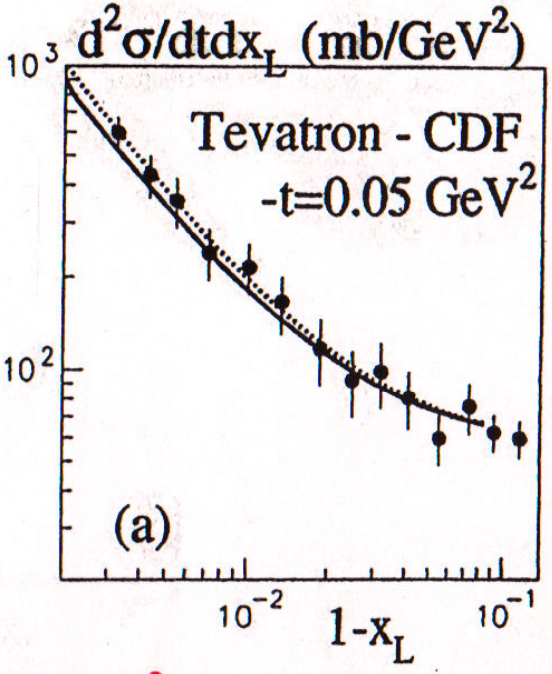

Pomeron enhancement is included in the package deal of $\mathbb{P}$ physics.
However, we do not have, as yet, a decisive direct experimental verification of this dynamic feature. Hopefully, LHC early measurement of σ_{tot} and σ_{el} will provide this support ahead of detailed M^2_{diff} measurements.

GLMM and KMR sum the Pomeron enhanced diagrams differently.

- GLMM MPSI summation has only enhanced diagrams neglecting the semi enhanced contributions. This implies a large deficiency in the calculation of high mass diffraction and was, thus, corrected by an explicit summation of the missing semi enhanced diagrams. The calculation of the survival probabilities, though, sums only over the MPSI terms.
- KMR summation neglects a significant part of the enhanced loop diagrams. Obviously, the two sets of calculations require an improvement!
- The above is at the core of the large difference between S^2_{enh} (GLMM) and S^2_{enh} (KMR). We distinguish between the eikonal re-scatterings of the initial projectiles resulting in a Gap Survival Probability (S^2_{2ch} in GLMM notation, S^2_{eik} in KMR notation) which is factorized from the final non GW diffraction.
- The above different summations are responsible for the large difference $\frac{S^2_{enh}(KMR)}{S^2_{enh}(GLMM)} \simeq 5\text{-}6$ in central diffraction.

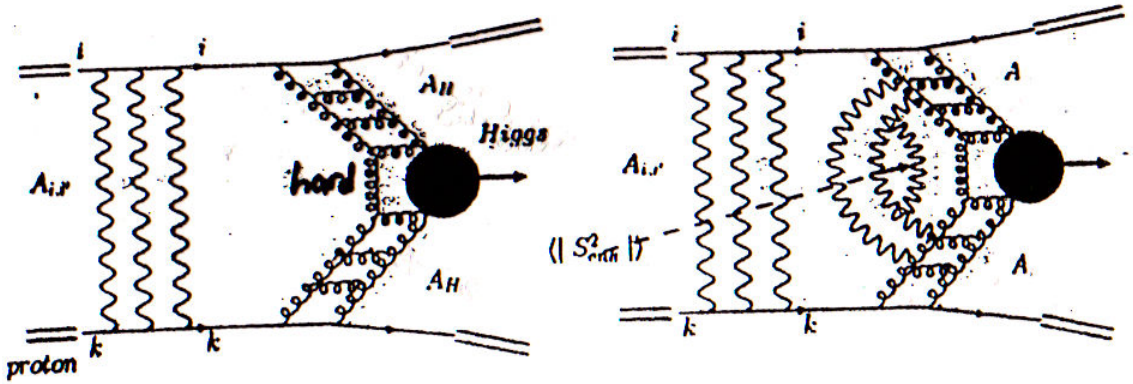

GLMM (08)

factorizable

The enhanced $\mathbb{P}$ interaction carries no memory of the initial hadron pdf

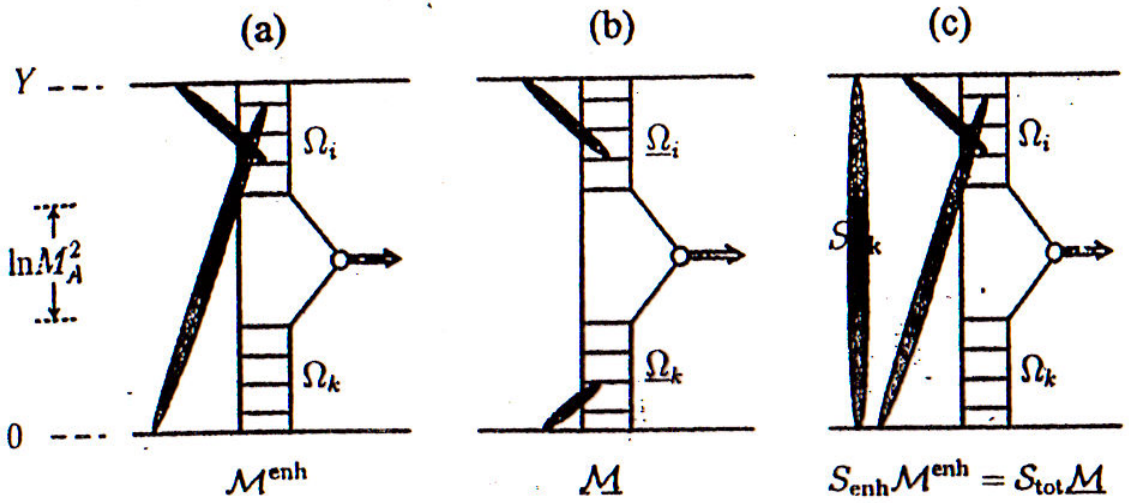

KMR (08)

non factorizable

The semienhanced interacting $\mathbb{P}$ is constraint by the initial state interacting $\mathbb{P}$ sharing the initial hadron pdf.

5. The Interplay Between Theory and Data Analysis

There is a significant difference between GLMM and KMR data analysis. This reflects on both the construction of the two data base sets and the coupled free parameters adjustment. The starting point of both investigations is the realization that a GW model reproduces the elastic data well, but the reproduction of the diffractive data is poor. Both groups claim to achieve a much improved reproduction of their respective data bases once $I\!P$-enhanced diagrams were added. The meager data in the $S_{p\bar{p}}S$ - Tevatron range is not sufficient to constrain the $I\!P$ parameters. GLMM(08) and KMR(09) chose, therefore, to extand their data base down to ISR ($W > 20$ Gev). This requires a $I\!P+I\!R$ fit from which one isolates the relevant $I\!P$ parameters. KMR (07,08) chose to tune rather than fit $\Delta_{I\!P}$ and $\alpha'_{I\!P}$ in a $I\!P$ only model.

GLMM data base has 55 points of σ_{tot}, σ_{el}, σ_{sd}, σ_{dd} and B_{el} in the ISR - Tevatron range. We add a consistency check of B_{sd} and $\frac{d\sigma_{el}}{dt}$ ($t \leq 0.5$ GeV^2), $\frac{d\sigma_{sd}}{dt\, d\frac{M^2}{s}}$ at $t = 0.05$ GeV^2 (CDF). The reason: we did not wish to bias the fit by too many differential cross sections points.

As stated, the GLMM fit was done twice, once for GW and

	$\Delta_{I\!P}$	β	$\alpha'_{I\!P}$	g_1	g_2	m_1	m_2	$\chi^2/d.o.f.$
GW	0.120	0.46	0.012 GeV^{-2}	1.27 GeV^{-1}	3.33 GeV^{-1}	0.913 GeV	0.98 GeV	0.87
GW+$I\!P$-enhanced	0.335	0.34	0.010 GeV^{-2}	5.82 GeV^{-1}	239.6 GeV^{-1}	1.54 GeV	3.06 GeV	1.00

TABLE I: Fitted parameters for GLMM(08) GW and GW+$I\!P$-enhanced models.

again for GW+ P-enh. As seen α'_P is very stable. The other free parameters change significantly. Noteably, Δ_P is much higher. This is a consequence of the additional constraints implied by the diffractive data which is more screened than the elastic sector. Another significant change is g_2(GW+P-enh.) $\simeq 40\, g_2$(GW). The conceptual approach of KMR is completely different. Their data base contains just:

$\frac{d\sigma_{el}}{dt}$ ($t \lesssim 0.5\ GeV^2$) in the 60–1800 GeV range.

The corresponding σ_{tot}.

CDF $\frac{d\sigma_{SD}}{dt\, d\frac{M^2}{s}}$ at $t \simeq 0.05\ GeV^2$.

In the KMR procedure the first stage is to fit/tune $\frac{d\sigma_{el}}{dt}$ including the consequent σ_{tot} so as to determine the b-profiles and the GW amplitudes. These are frozen and utilized in the second stage in which Δ_P, α'_P are determined.

KMR (00) GW

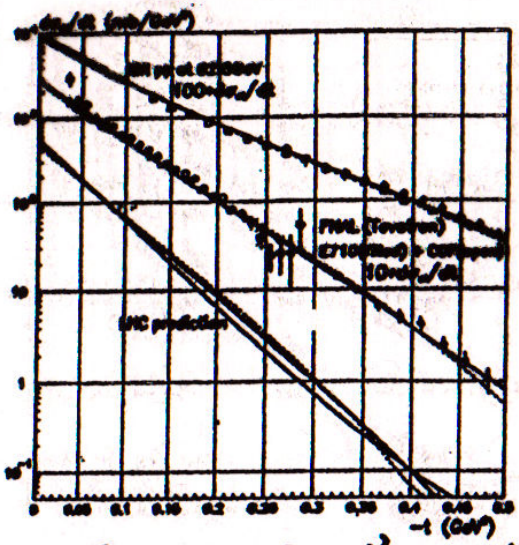

$\Delta_{I\!P} = 0.102$ $\alpha'_{I\!P} = 0.066$

RMK (07)

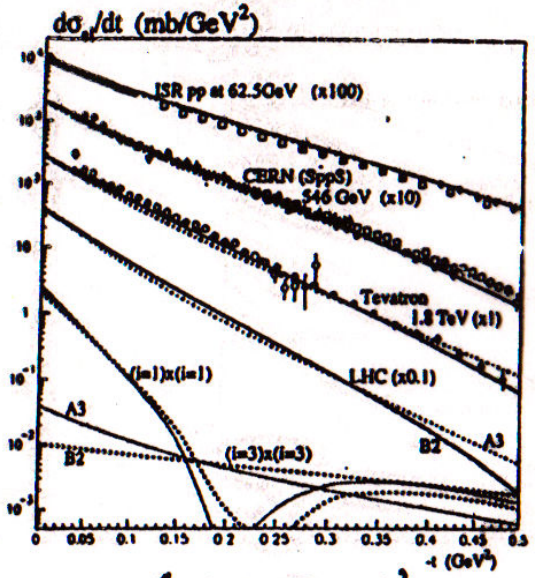

$\Delta_{I\!P} = 0.55$ $\alpha'_{I\!P} \equiv 0$

RMK (08)

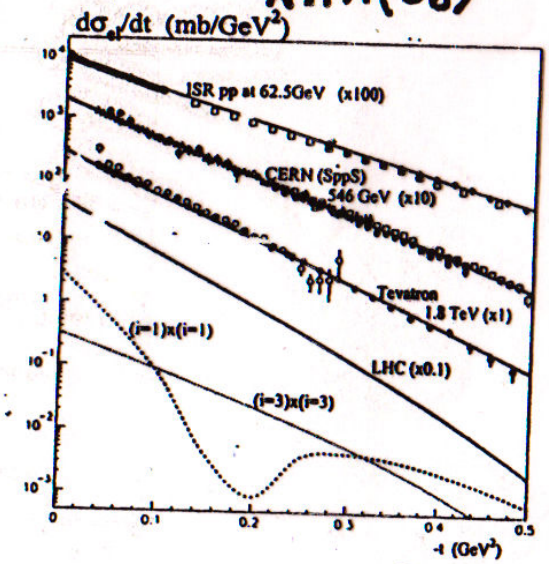

$\Delta_{I\!P} = 0.30$ $\alpha'_{I\!P} = 0.05$

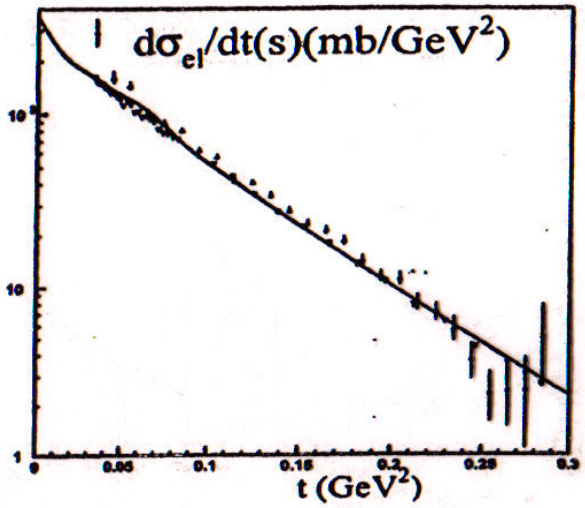

GLMM (08) GW

$\Delta_{I\!P} = 0.12$

$\alpha'_{I\!P} = 0.012$

GLMM (08) GW+Penh

$\Delta_{I\!P} = 0.335$

$\alpha'_{I\!P} = 0.010$

LKMR (08)

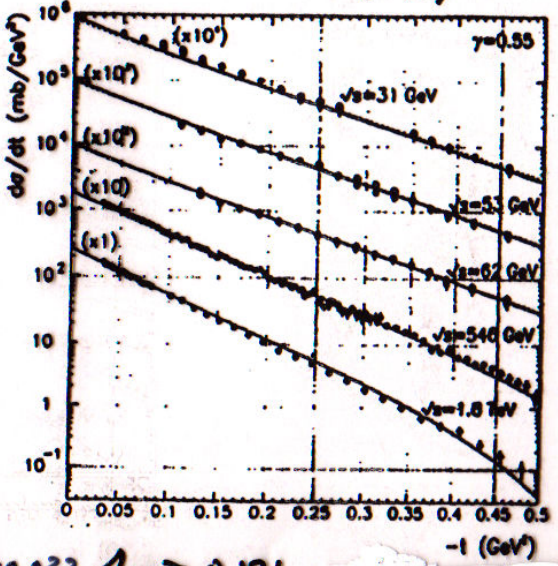

$\alpha'_{I\!P} = 0.033$ $\Delta_{I\!P} = 0.121$

$1 - X_L = \frac{M_{cd}^2}{s}$

GLMM (08) $\mathbb{P}$ enhanced + GW

$\Delta_{\mathbb{P}} = 0.335 \quad \alpha'_{\mathbb{P}} = 0.010$

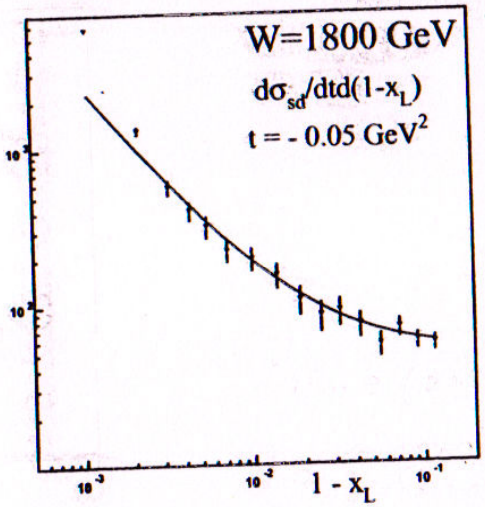

LKMR (08)

GW +

Mueller's 3$\mathbb{P}$ SD

only

$\Delta_{\mathbb{P}} = 0.121 \quad \alpha'_{\mathbb{P}} = 0.033$

KMR (07)

$\mathbb{P}$ enhanced + GW

$\Delta_{\mathbb{P}} = 0.55 \quad \alpha'_{\mathbb{P}} \equiv 0$

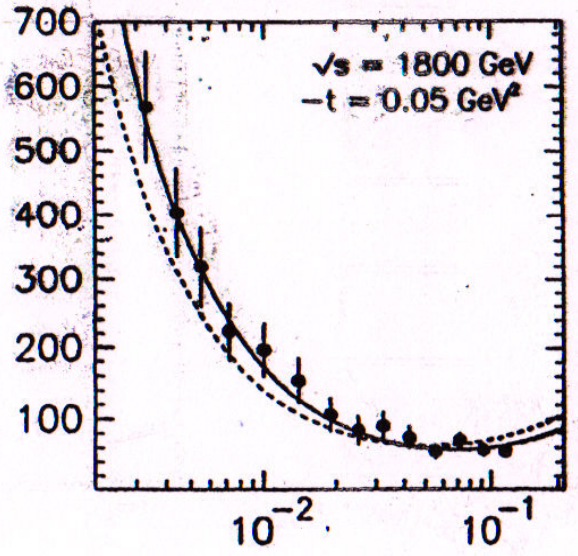

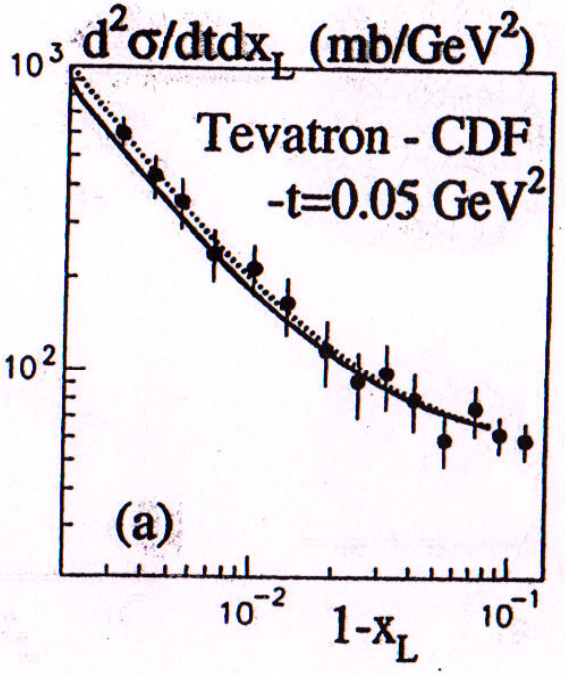

One of the consequences of the KMR procedure is that g_1 and g_2 are of the same order (compatible with GLMM first phase fit). As we shall see this output is critical in the study of the approach of $a_{el}(s,b)$ to the black disc bound.

Some, but not all, of the deficiencies of the KMR data analysis are amended in LKMR(09) in which both $I\!P + I\!R$ exchanges are included enabling a larger data base containing the ISR – Tevatron data. Recal, though, that LKMR have adopted the KMR approach and their data base contain only $\frac{d\sigma_{el}}{dt}$, σ_{tot} and $\frac{d\sigma_{sd}}{dt\, d\frac{M^2}{s}}$.

In my oppinion fitting $\frac{d\sigma_{el}}{dt}$ on its own is no more than a consistency check. KMR and LKMR data analysis has no resolution to determine the $I\!P$ parameters and the GW scattering amplitudes.

The extensive LKMR(09) analysis of $\frac{d\sigma_{sd}}{dt\, d\frac{M^2}{s}}$ convincingly demonstrates the need to supplement the 3$\mathbb{P}$ vertex with secondary Regge Contributions such as $\mathbb{P}\mathbb{P}\mathbb{R}$ and $\mathbb{R}\mathbb{R}\mathbb{P}$. However, LKMR model does not address the $\mathbb{P}$ enhancement contribution. As such this analysis has very limited relevance in our context.

Once again, the less extensive analysis of KMR(07) and GLMM(08) is a consistency check as both model need an arbitrary background term to reproduce the CDF data. Note, also, that LKMR were able to fit the CDF $\frac{d\sigma_{sd}}{dt\, d\frac{M^2}{s}}$ at 540 and 1800 GeV only after a relative normalization rescale of 25%.

To conclude: in as much as I admire KMR for their intuition, I do not think that their data analysis provides convincing support to their theoretical assumptions and numerics of their parameter choice.

6. The Approach Toward the Black Disc Bound

The unitarity bound $|A_{i,k}(s,b)| \le 2$ holds if $\Omega_{i,k}(s,b)$ is arbitrary. In the eikonal model $\Omega_{i,k}$ is real, i.e. $A_{i,k}(s,b)$ is imaginary. The small real part of $A_{i,k}(s,b)$ can be calculated utilizing dispersion relations (Cauchy theorem). In this case the unitarity bound coincides with the black disc bound $|A_{i,k}(s,b)| \le 1$.

It is easy to see that $A_{i,k}(s,b) = 1$ if and only if

$$A_{1,1}(s,b) = A_{1,2}(s,b) = A_{2,2}(s,b) = 1.$$

This implies that $a_{el}(s,b) = 1$ while $a_{sd}(s,b) = a_{dd}(s,b) = 0$.

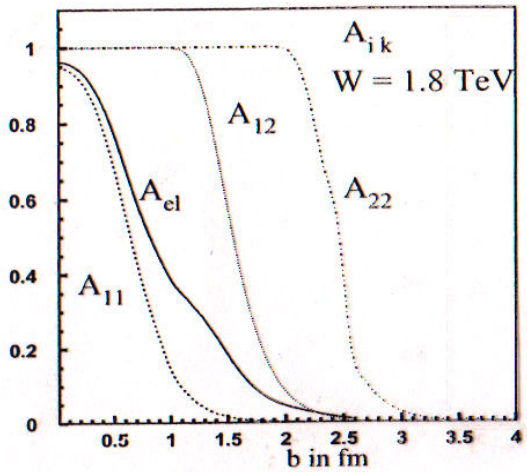

Fig. 14-a

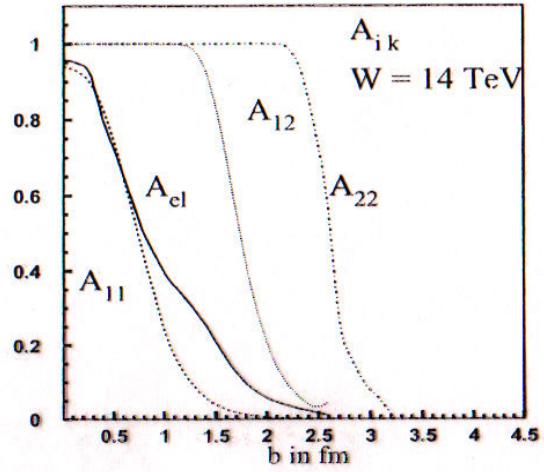

Fig. 14-b

Figure 14: Impact parameter dependence of $A_{i,k}$ and a_{el} at different energies.

As a result the integrand of the convolution defining $S^2_{2ch}(s)$ at this b vanishes

$$S^2_{2ch}(s,b) = 0$$

The interest in the rate at which $a_{el} \to 1$ at small b is obvious as a feature of conceptual interest. Lets discuss its details.

- Recall that if $a_{el}(s,b) = 1$ all diffractive channels (soft or hard) vanish at this (s,b) point, be it a consequence of the GW mechanism properties or because $S^2_{2ch}(s,b) = 0$.
- Checking the GLMM(08) fitted parameters it is clear that since $g_2 \gg g_1$, $A_{2,2}(s, b=0)$ reaches unity at relatively low energies, $A_{b2}(s, b=0)$ reaches unity at medium $W \simeq 100$ GeV and $A_{1,1}(s,b=0)$ will reach unity at exceedingly high energies well above LHC. So would $a_{el}(s, b=0)$.
- In KMR(08) $g_1 \simeq g_2$ and consequently in this model $a_{el}(s, b=0)$ will reach unity just above the LHC energy.
- We expect that even though σ_{tot} and σ_{el} as calculated by the two models at LHC and Auger are comparable $S^2_{2ch}(GLMM) > S^2_{2ch}(KMR)$. Recall, that the adjusted values of $A_{i,k}$ are determined in GLMM(08) by a fit to a GW + $I\!P$-enh. model.

The behaviour of $R_D = \frac{\sigma_{el} + \sigma_{sd} + \sigma_{dd}}{\sigma_{tot}}$ conveys information on the onset of s-unitarity constraints at high energies. Assume that diffraction originated exclusively from the GW mechanism. We obtain then the Pumplin bound: $R_D \leq \frac{1}{2}$. The non GW multi Pomeron induced diffractive contributions are not included in the Pumplin bound since they originate from $G^{in}_{i,k}$ rather than from $A_{i,k}$. As such they are reduced from their non screened calculated rates by the corresponding survival probability. The delicate balance between the increase of the non screened cross section and the decrease of S^2 with energy is **model dependent**. In GLHM(08) $R_D < 0.5$ decreasing slowly with energy. In KMR(07) $R_D > 0.5$ increasing slowly with energy up to $W = 10^5$ GeV which is the high energy limit of validity for both KMR and GLHM. The origin of the KMR prediction is the relatively fast increase of high mass diffraction.

7. Concluding Remarks

1) A primary implication of Pomeron enhancement is that σ_{tot} and σ_{el} are reduced at LHC and above. Both GLMM and KMR predictions are 10-20% lower than estimated 2 years ago.
2) A measurement of σ_{sd} and σ_{dd}, in particular high mass, is critical for the understanding of Pomeron enhancement and its decisive verification.
3) I wish to end with a common sense reminder. Obviously, any reasonable model applied to the multi Tev range is required to reasonably reproduce the $S p\bar{p}S$-Tevatron data. It is also obvious that this is not sufficient.
To remind you, the range of "legitimate" σ_{tot} predictions at the LHC spreads from 90 mb (GLMM, KMR) to 280 mb (Troshin and Tyurin).